

# Deformation of High-Density Polyethylene Produced by Rolling with Side Constraints. I. Orientation Behavior

Z. Bartczak

Centre of Molecular and Macromolecular Studies, Polish Academy of Sciences, Sienkiewicza 112, 90-363 Lodz, Poland

Received 25 April 2001; accepted 7 February 2002

**ABSTRACT:** A new method of rolling with side constraints was applied to polyethylene. The process relies on the rolling of a material inside a channel formed on the circumference of one roll with another roll having a thickness matching the width of the channel in the first roll. The rolling inside a channel resembles to a large extent the plane-strain compression in a channel die. The deformation processes of linear polyethylene by compression in a channel die and by rolling with side constraints proceed in very similar fashions and produce similarly strong single-component crystal textures accompanied by chevronlike lamellar

structures at comparable strains. The macromolecular chains are highly oriented along the rolling direction. At high rolling rates, {310} twinning takes place with both the channel die and rolling with side constraints because of tensile stress across the bar caused by strain recovery on unloading. The constraint rolling allows for the production of bars or profiles with relatively large cross sections ( $>1 \text{ cm}^2$ ) in a continuous manner. © 2002 Wiley Periodicals, Inc. *J Appl Polym Sci* 86: 1396–1404, 2002

**Key words:** orientation; polyethylene (PE); structure

## INTRODUCTION

Preferred molecular orientation is one of the advantageous results of the plastic deformation of polymeric materials. In most cases, it leads to an increase in a material's toughness and strength. The permanent deformation of polymeric materials can be achieved by numerous different methods, such as uniaxial and biaxial tension, uniaxial compression, plane-strain compression, rolling, solid-state extrusion, and combinations of drawing with rolling or hydrostatic compression.<sup>1–4</sup> The most common method of deformation used in both laboratory and industrial practice is simple drawing.

It is often observed that the plastic deformation of crystalline polymers, especially that produced by cold drawing, causes a significant amount of cavitation. One of the visible marks of cavitation is sudden polymer whitening near the yield point. Galeski et al.<sup>5</sup> demonstrated with a transmission electron microscopy investigation of polyamide-6 that the cavities are formed in the bulk of polyamide during plastic deformation and that they are preferentially located at points of mechanical mismatch of adjacent stacks of lamellae. The cavitation is associated with massive chain scission and is an intense phenomenon in several bulk polyamides.

The internal cavitation of the type observed in tensile experiments has been called *micronecking* by Peterlin.<sup>6</sup> It had been considered for a long time to be an essential mechanism allowing large strain deformation of aggregates of chain-folded crystals. It was thought that it removed kinematic constraints between lamellae and allowed them to untangle. Although this picture looks reasonable in tensile deformation, it is flawed for other deformation modes, which do not produce cavitation, such as compression, in which a positive normal stress component prevents any cavitation. It has been shown that micronecking is inessential for the development of nearly perfect single-crystal textures for several semicrystalline polymers that result from high plane-strain compression in a channel die.<sup>7–10</sup> Although plane-strain compression is kinematically very similar to drawing, cavitation does not occur because of the positive normal stress component. Numerous observations have confirmed that the crystalline and associated amorphous regions of the material undergo a continuous series of shear-induced morphological transformations without any cavitation process.

Among other known methods of plastic deformation, rolling is one of the best ways to produce a high preferred orientation.<sup>11–13</sup> Like compression, cavitation is usually not observed with rolling because of a high compressive stress component. Rolling is an attractive method of plastic deformation from an industrial point of view because it can be designed as a continuous process. However, the force required to roll significantly a wide strip of polymeric material sometimes rises unacceptably high, whereas for nar-

Correspondence to: Z. Bartczak (bartczak@bilbo.cbmm.lodz.pl).

row strips there is an unwanted component of transverse deformation deteriorating the final texture and, therefore, the properties of the oriented material. Side effects of transverse deformation also include the formation of fissures, cracks, and cavitation at the edges of a rolled material. These phenomena limit the use of rolling to the production of only relatively thin products in the form of films, thin sheets, or tapes.

So that the limitations of conventional rolling might be overcome, a novel method of obtaining highly oriented polymeric materials was developed recently in our laboratory. This method of rolling with side constraints<sup>14,15</sup> is a combination of channel-die compression and rolling. This process relies on the rolling of a material inside a channel formed on the circumference of one roll with another roll having a thickness matching the width of the channel in the first roll. The idea of constraint rolling is depicted in Figure 1. The side walls of the channel on the roll constitute lateral constraints as for channel-die compression. The other roll plays a role similar to that of plunger. The system of rolls with a channel develops conditions close to plane-strain compression of the rolled material. That deformation mode is known to produce a well-developed single-component texture (quasi-single-crystal) of compressed materials.<sup>7</sup> The advantage of such constrained rolling is the possibility of large strain deformation of relatively thick and wide and infinitely long bars or profiles in a continuous manner. The resulting profiles may have considerably high cross-section areas and superior mechanical properties comparable to those of fibers.

In this article, studies of the development of the orientation of high-density polyethylene during rolling with side constraints are reported. Orientation produced by constrained rolling is compared with that obtained by plane-strain compression in a channel die to show the correspondence of both deformation processes.

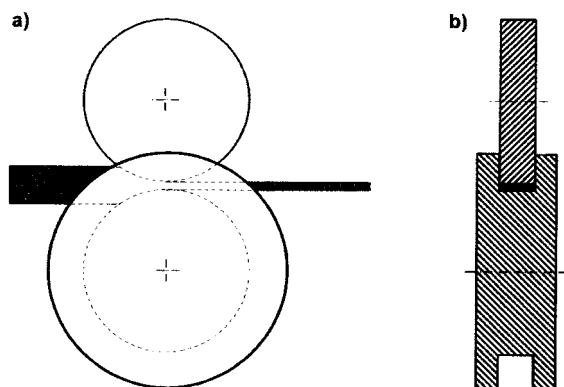


**Figure 1** Scheme illustrating the principle of rolling with side constraints.

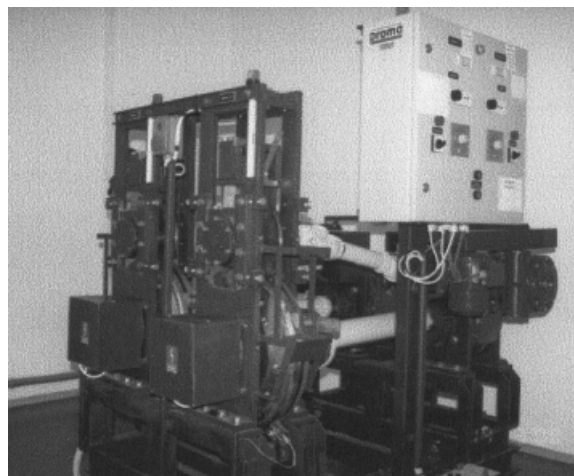


**Figure 2** View of the laboratory four-roll rolling apparatus.

## EXPERIMENTAL

### Rolling apparatus

The prototype apparatus, shown in Figure 2, consists of two sets of rolls, similar to those shown in Figure 1, made of surface-hardened steel with an effective (working) diameter of 280 mm. The lower roll in each set has an outer diameter of 480 mm and a channel cut into the circumference to a depth of 100 mm and to a width of 12 mm. The coworking upper roll has a diameter of 280 mm and a width of 12 mm, matching the channel in the lower roll. The spindles and base of the machine were designed to be sturdy enough to resist expected very high loads. In each set, the spindle of an upper roll is mounted to the frame through a movable slide. The position of the upper roll against the lower and, therefore, the amount of desired compression on rolling are set by a screw attached to the slide. A load cell for measurements of the force exerted on the rolled material can be fitted between that screw and the slide. The temperature of the rolls is controlled independently for both sets of rolls by temperature controllers connected to flat heaters mounted on both sides of the lower rolls. Each set of rolls is driven independently by electric motors through two-speed gear boxes; this results in two selectable rolling rate ranges: up to 500 mm/min and up to 4200 mm/min. Because the speed of both roll sets is controlled independently, the apparatus allows us to combine rolling with axial deformation; the rolled bar can be either pulled out or pushed into the rolling zone by the other roll set (i.e., rolled and drawn or compressed and rolled simultaneously).

### Materials and procedures

Two high-density polyethylene resins were used in this study. One was a PE-80 pipe grade (Finathene

HP-401, Atofina (Paris); melt-flow index = 0.51 g/10 min at 5 kG and 190°C, density = 0.95 g/cm<sup>3</sup>, filled with less than 3 wt % carbon black), and the other was a high molecular mass medium-density polyethylene (DSM, Geleen, The Netherlands; melt-flow index = 0.46 g/10 min at 5 kG and 190°C, density = 0.945 g/cm<sup>3</sup>, delivered in the form of sheets 12.5 mm thick); they are labeled throughout this study PE-1 and PE-2, respectively. The slabs, 100 mm × 12 mm and 1 m long, were machined out from either a thick-wall pipe (PE-1) or a sheet (PE-2).

The rolling of specimens was performed on the apparatus described in the previous section. The rolling speed was set to 200 or 4000 mm/min (the same for both sets of rolls), and the temperature of the rolls was 25, 90, or 110°C. The polyethylene slabs were preheated to the desired temperature before the rolling. Samples were deformed by being rolled to various deformation ratios (DRs), defined as the ratios of the initial and final cross sections of the sample, from DR = 2 to DR = 8.3. For higher DRs, it was necessary to roll a slab in several subsequent passes of smaller DRs.

For reference, the samples of the same materials were compressed in a channel die described in previous articles<sup>7,9</sup> at temperatures and deformation rates comparable to those applied in the rolling experiments.

The texture of the rolled and compressed samples was studied with the X-ray pole figure technique (for an overview of this technique, see ref. 16). A wide-angle X-ray scattering system consisted of a computer-controlled pole figure attachment associated with a wide-angle goniometer coupled to a sealed-tube source of filtered Cu K $\alpha$  radiation operating at 30 kV and 30 mA. The details of the technique of pole figure preparation are described elsewhere.<sup>7</sup> The following diffraction reflections from the orthorhombic crystal form of polyethylene were analyzed: (110), (200), (020), and (002).

Lamellar orientation was probed by two-dimensional small-angle X-ray scattering (2D SAXS). A 1.1-m-long Kiessig-type camera was equipped with a pin-hole collimator and an imaging plate as a recording medium (Eastman Kodak, Rochester, NY). The camera was coupled to an X-ray generator (sealed-tube, fine-point Cu K $\alpha$ -filtered source operating at 50 kV and 35 mA; Philips, Eindhoven, The Netherlands). Exposed imaging plates were read with a PhosphorImager SI system (Molecular Dynamics, Sunnyvale, CA).

The melting behavior of oriented samples was characterized with a Thermal Analysis TA 2100 differential scanning calorimeter (New Castle, DE). The 5–8-mg specimens were cut from oriented samples in the plane perpendicular to the flow direction. As a reference, a sample of unoriented polyethylene with a similar thermal history was also investigated. The differ-

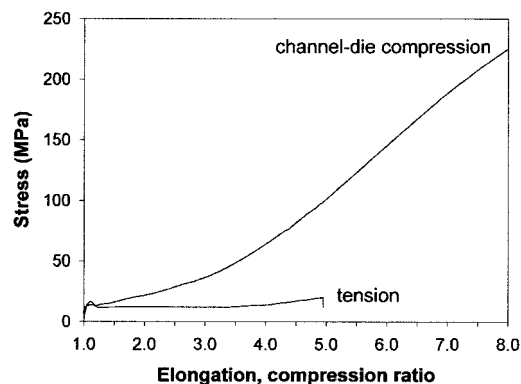


**Figure 3** Stress–strain curves of PE-2 samples deformed by compression in a channel die at 90°C and in tension at room temperature.

ential scanning calorimetry (DSC) scans were made at a heating rate of 10°C/min.

## RESULTS AND DISCUSSION

An usual side effect of the plastic deformation of a semicrystalline polymer by simple drawing with no or few side constraints is cavitation. In deformation by compression, cavitation is less likely because of positive normal stresses. However, side constraints imposed on the material in compression prevent any cavitation.

The presence of side constraints completely changes the process of plastic deformation in compression: no neck is formed, and although the yield stress remains at a similar level in comparison with tension, further deformation of the polymer leads to dramatically higher loads. This is illustrated in Figure 3, in which stress–strain curves for high-density polyethylene deformed in tension and plane-strain compression in a channel die (i.e., with constraints) are compared. The material responds to compression with a stress of nearly 250 MPa. For comparison, when there are no constraints in the tensile deformation mode, intense cavitation leads to the ultimate strength of merely 30 MPa (see Fig. 3), and fracture occurs by a sequential break of single microfibrils. Moreover, the drawn cavitated material has little transverse strength because of loose connections between microfibrils formed during tensile deformation.

The rolling of bars of PE-1 and PE-2 was performed in the rolling apparatus with a linear speed of 200 mm/min at room temperature, 90°C, and 110°C. Neither necking nor cavitation phenomena were observed for rolling under these conditions. Deformation was homogeneous in the entire strain range studied, as observed for compression in a channel die. Samples of PE-2 with the DR approaching 4 became translucent, unlike the opaque bars of virgin PE-2. This transfor-

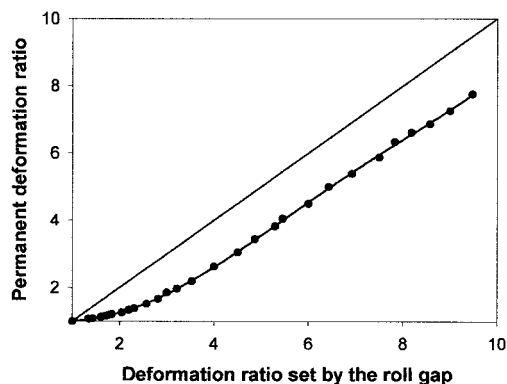


**Figure 4** Dependence of the permanent strain on the strain imposed on the sample during rolling, with both expressed in terms of DR.

mation could not be observed for PE-1 samples because PE-1 was filled with carbon black. The force exerted on the rolls increased greatly with the increase in the DR, despite the continuous reduction of the cross section of the rolled material. Measurements of the force generated on the upper roll at several DRs suggested that the stress-strain curve for rolling was quite similar to that observed in channel-die-compression experiments. No fracture of the samples was observed even with heavy rolling up to a DR around 6. Rolling to higher strains, especially between DR = 7 and DR = 8.3, caused, however, some limited fracture of the material along the rolling direction (RD), which sometimes led to a partial delamination of the rolled bar in planes close to the rolled surface (i.e., the surface in contact with the upper roll). These phenomena could be observed especially in PE-2 samples, whereas PE-1 was more resistant to fracture under those deformation conditions. A tendency to fracture at large strains was stronger at low temperatures for the deformation process.

The rolling of polyethylene at a speed of 4 m/min was performed at room temperature and 90°C sequentially with several steps of lower deformation up to the final DR of 7. Rolling to higher deformations led to the fracture and eventual breaking of the rolled samples. The fracture usually started close to the rolled

surfaces of the bar and then developed deeper into the bar, eventually causing the breaking of the entire sample. As for rolling at a low speed, the fracture occurred more easily when rolling was performed at room temperature than at 90°C.

The rolled samples demonstrated substantial strain recovery after leaving the deformation zone between rolls. This strain recovery was short-term and ceased approximately at a distance of 20 cm or less beyond the roll, depending on the temperature and deformation rate. Figure 4 presents the permanent strain plotted against the actual strain achieved within the deformation zone between rolls. The strain recovery increases with increasing DR up to a DR between rolls of nearly 4 and then saturates and remains constant with a further strain increase. Such behavior indicates the presence of some quasielastic component within the structure of the rolled material, which apparently was not destroyed even by heavy rolling. This is discussed further in this section. Such strong strain recovery was not observed previously in the compression of linear polyethylene in a channel die.<sup>7</sup> However, similar recovery behavior was observed in channel-die-compressed samples of ultrahigh molecular weight polyethylene.<sup>10</sup> The polyethylene used in this study had a relatively high molecular weight, in the range of half a million, and so its postdeformation behavior was more similar to that of ultrahigh molecular weight polyethylene<sup>10</sup> than to that of linear polyethylene with a weight-average molecular weight  $M_w = 55,000$ .<sup>7</sup>

The undeformed slabs were imprinted with evenly spaced linear markers perpendicular to the RD before the rolling. The distance between markers was measured after each rolling pass. The macroscopic strain calculated from that distance between markers correlated well with that calculated from the reduction of the cross section of the rolled sample. The evolution of the shape of the markers with increasing strain can illustrate the macroscopic flow within the sample and can be an indication of the changes in the local strain across the rolled slab. The shape of the markers at various DRs is shown in Figure 5. This figure illustrates that the rolling leads to a nearly pure compress-

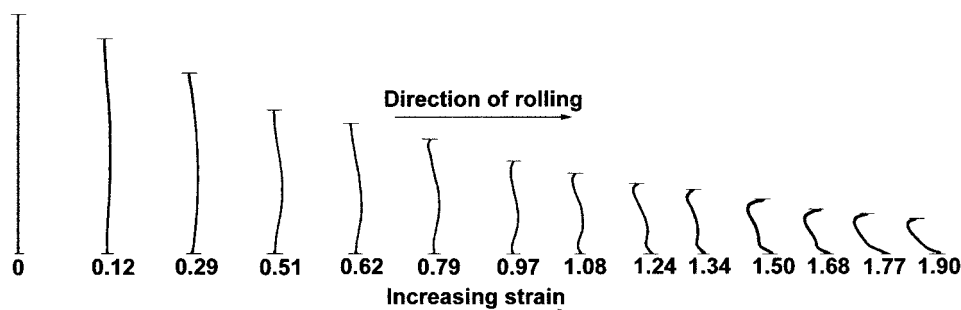


**Figure 5** Shape of the markers after rolling to the true strain indicated [ $\epsilon = \ln(\text{DR})$ ].

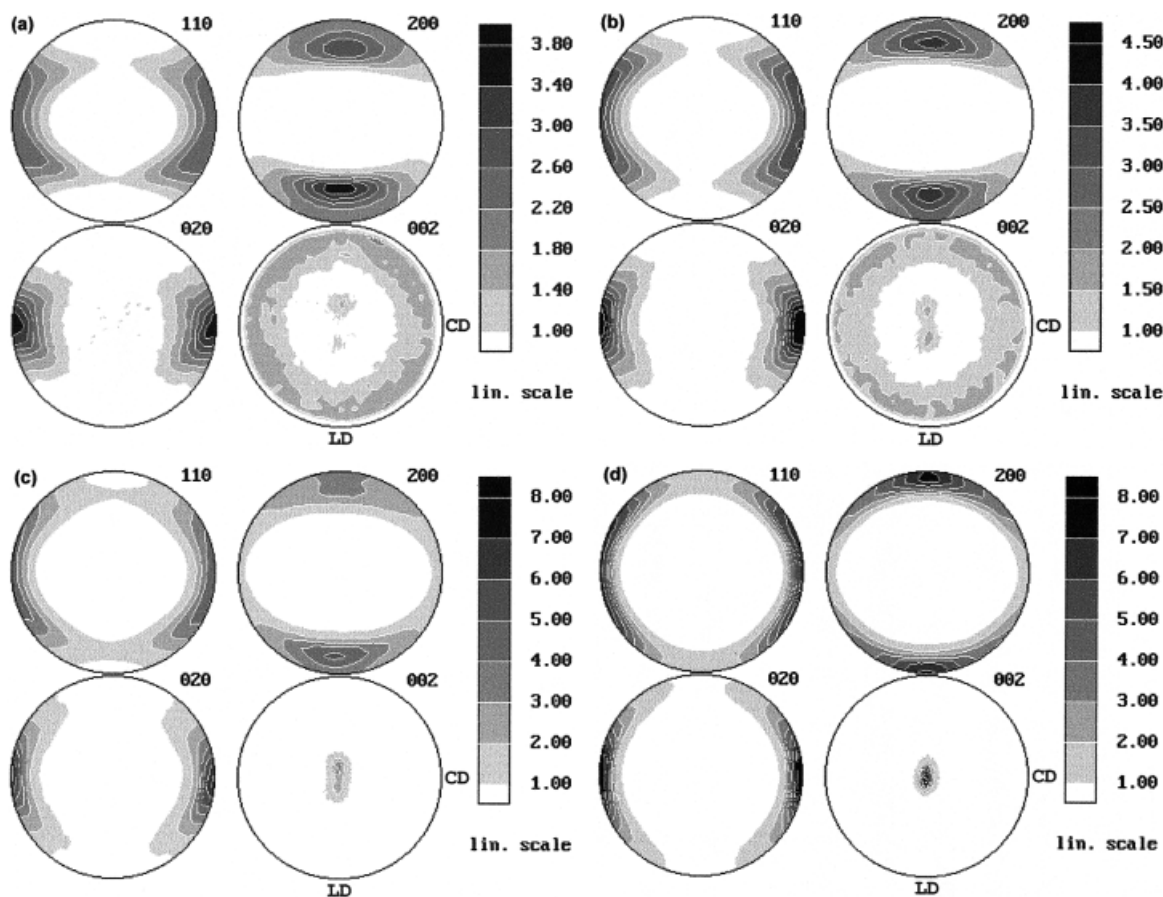


**Figure 6** Pole figures of the (110), (200), (020), and (002) planes of orthorhombic polyethylene determined for samples of PE-2 rolled at 110°C with a roll speed of 200 mm/min to the DR of (a) 2.1, (b) 2.7, (c) 3.5, (d) 4.9, (e) 6.4, (f) 7.4, (g) 8.3.

sion, with only a little macroscopic shear manifesting in a weak flow along the rolling direction (RD), especially in the range of low DRs. Such shear produces a slightly higher strain in the central part of the bar than near its rolled faces. However, with an increasing DR, the profile of markers becomes curved and extends in the RD in the vicinity of both rolling faces. This supports a shear component, increasing with an increase in the overall strain. The shear and, therefore, flow are strongest near the rolled faces. Consequently, at high DRs, a higher local strain develops in the material near the rolled faces of the bar than in its central part. These differences in the local strain are responsible for premature fracture of the bar occurring near rolled surfaces at high DRs, as reported previously. The development of shear in the range of high strain results from a decreasing friction force at side walls of the channel with increasing DR because of the reduction in the thickness of the rolled bar. At the same time, the area of rolled surfaces and, therefore, the friction force against the rolled surfaces remain constant (this friction is, in fact, a driving force of the rolling process), whereas the compressive stress within the material rises substantially with an increasing strain. Consequently, at a certain DR, the total friction force (against

sides and rolled faces of the sample) is no longer high enough to maintain the deformation rate of the sample set by the rotating rolls, and the rolled bar slows down relative to the rolls. However, the friction on the rolled faces of the sample is still sufficient to produce some shear deformation of the material close to that surface, which results in somewhat higher local strain being produced near rolled surfaces than in the center of the bar.

Figure 6 presents the pole figures of the basic crystallographic planes of samples of PE-2 rolled at 110°C and at a speed of 200 mm/min to various DRs up to 8.3. This figure demonstrates the continuous development of a sharp, single-component texture of the (100)[001] type, that is, a quasi-single-crystal texture with the chain axis (i.e., [001] direction, normal to the (002) plane) aligned well along the RD and the (100) plane oriented with its normal along the loading direction (LD). The pole figures obtained for samples of PE-1 rolled under similar conditions are very similar and, therefore, are not presented here. The single-component texture observed at high strain results from a merge of two texture components, both oriented with their [001] directions at some acute angle against RD. They appear clearly at a relatively low

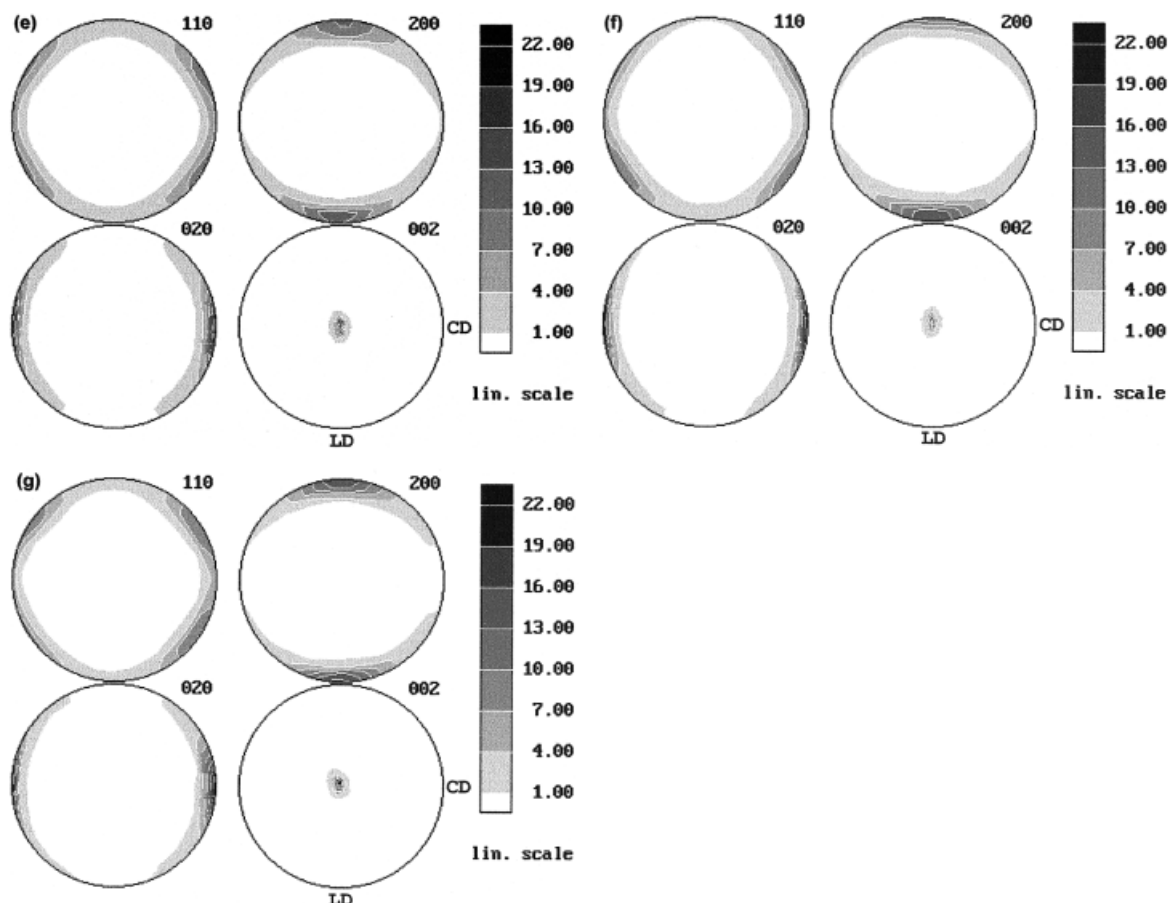


Figure 6 (Continued from the previous page)

strain of nearly 2, approximately  $20^\circ$  away from the RD toward the LD. With increasing strain, the tilt angle of the (001) direction of both components decreases with respect to RD, whereas the overall texture intensifies and sharpens substantially. Finally, at a DR above 5, both components merge into a single component, which then sharpens even more with a further increase in the DR.

This sequence of formation of the final texture follows nearly exactly the evolution of the texture of high-density polyethylene deformed by plane strain in a channel die, as reported in ref. 7. It indicates that the deformation process and mechanisms involved are very similar in both deformation modes.

Figure 7(a) shows the pole figures determined for a sample of PE-1 rolled to the permanent DR of 7 at the high rate of 4 m/min and at  $90^\circ\text{C}$ . In contrast to the previously described samples rolled at a low rate, the texture of this sample consists of three components. One of them is the same (100)[001] element reported previously, whereas other two are rotated by  $\pm 53^\circ$  around the RD [clearly seen in the (110), (200), and (010) pole figures in Fig. 7(a)] but maintain the chain direction along the RD [as demonstrated by the (002) pole figure in Fig. 7(a)]. The clustering of normals to (200) planes at  $\pm 53^\circ$  coincides with the position of

(310) poles for the (100)[001] texture component and clearly indicates that these new texture components resulted from {310} twinning of the basic (100)[001] component. Such twinning had to occur on unloading, when the sample left the deformation zone between the rolls. The partial recovery of the strain reported earlier in this section produces a tensile stress along the LD. It was demonstrated earlier that such oriented tensile stress could induce a {310} twinning in orthorhombic polyethylene.<sup>17</sup> The other stress that could induce observed {310} twinning is a compressive stress in the direction close to the constraint direction (CD). However, such compressive stress can not be generated either during rolling with side constraints or during unloading and recovery.

Because no such twinning was observed previously in plane-strain-compression experiments, some additional compression tests with various deformation rates were performed to determine whether such twinning was specific to the high-rate rolling alone or could also be induced in plane-strain-compression tests. The strain rate in compression tests was set within a range of 0.5–50 mm/min (the strain rates for stepwise rolling with the rolling speed of 4 m/min correspond approximately to the upper limit of that range). An exemplary set of pole figures determined

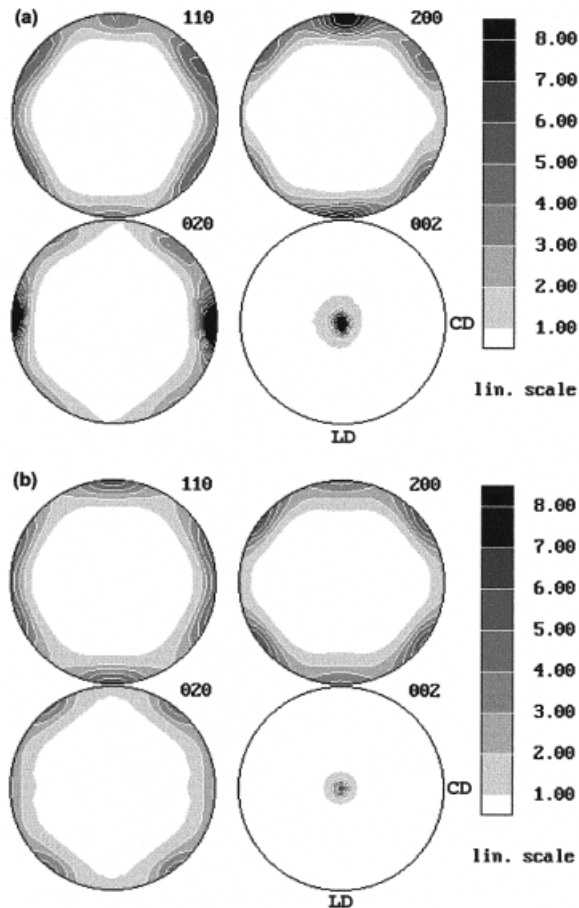


**Figure 7** Pole figures of the (110), (200), (020), and (002) planes of orthorhombic polyethylene determined for samples of PE-1 (a) rolled at 90°C with a roll speed of 4 m/min to a DR of 6.5 and (b) compressed in a channel die at 90°C with a deformation rate of 50 mm/min to a DR of 6.5.

for the sample of PE-1 deformed in a channel die with a strain rate of 50 mm/min is shown in Figure 7(b). The texture that developed under such deformation conditions shows the same features observed in the high-speed rolled sample. An examination of the texture of samples deformed in a channel die over a range of deformation rates demonstrates a continuous increase in the intensity of {310} twinning with an increasing deformation rate: twinning does not appear for deformation at a low rate, whereas it is substantial when the deformation rate is high. Figure 8, presenting azimuthal scans of the (200) reflection [equivalent to the trace of the (200) pole figure along its circumference], clearly demonstrates this finding. The aforementioned results indicate once more a close resemblance of the deformation behavior in compression and rolling, both in plane-strain conditions because of side constraints imposed.

Twinning is activated at high strain rates (i.e., higher rolling speeds) because in the samples deformed at lower rates the strain recovery process does not generate a tensile stress along the LD high enough

to involve twinning. It has been estimated that the critical resolved shear stress in the twin plane to activate twinning is around 14 MPa.<sup>18</sup> Therefore, the tensile stress generated along the LD on unloading must be at least 28 MPa. Such stress apparently generates with unloading only when a high deformation rate is applied during deformation.

Figure 9 presents 2D SAXS patterns of samples of PE-2 deformed through rolling to various permanent DRs. For every sample, two patterns are shown: one was recorded with an X-ray beam illuminating the sample along the LD, whereas the other was recorded with the beam along the CD. The LD-view pattern obtained for the sample deformed to the permanent DR of 2.1 is a superposition of an ellipse, elongated in the RD, and a little stronger two-point pattern oriented in RD. For higher DRs, the elliptical part of the pattern fades away, whereas the two-point component becomes stronger. Above a DR of 3, only the strong two-point signature is present in the LD-view pattern. The CD-view patterns are more complex. At DR = 2.1, that pattern consists of two long arcs oriented in the RD, a diffuse two-point pattern also oriented in the RD, and a four-point pattern. For DR = 2.7, the arcs become shorter, whereas the points of the two-point component elongate in the direction parallel to the LD. The four-point component is hardly seen for this deformation. At higher deformations of DR = 3.5 and 4.9, the CD-view pattern evolves further toward two lines oriented along LD. Along these lines, four clear maxima can be distinguished. This means that these patterns can be classified as the four-point type. For samples with DR = 6.4 and 8.3, clear four-point patterns are seen. Moreover, in the pattern of the sample rolled to DR = 8.3, four second-order maxima can be clearly observed. The presence of these maxima demonstrates a high degree of ordering of the lamellar structure.

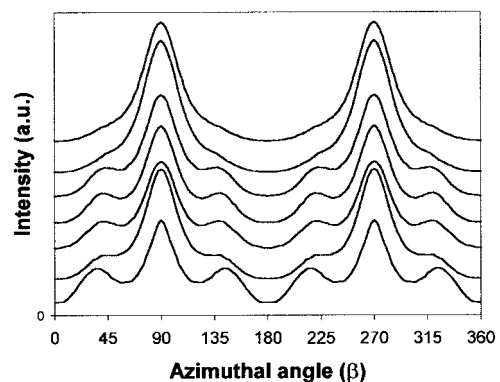


**Figure 8** Azimuthal scans of the (200) reflection along the circumference of the respective pole figure determined for samples of PE-2 compressed in a channel die at 90°C to a DR of about 6.5 with deformation rates of 0.5, 1, 2, 5, 10, 20, and 50 mm/min, respectively (from top curve to bottom curve).

The 2D SAXS patterns obtained for samples of rolled PE-1 show the same features as those reported previously, although they contain in addition an isotropic diffuse scattering from carbon black particles, which were dispersed in PE-1 samples. Because of the similarity to the patterns of PE-2 samples, these patterns are not shown here.

The 2D SAXS patterns of rolled samples described here are comparable to those reported previously for samples of conventionally rolled polyethylene<sup>11-13</sup> and differ from the channel-die-compressed samples, especially in the patterns recorded in the CD view, which consisted of two broad lines instead of four points.<sup>7</sup> The presence of a line pattern in channel-die-compressed polyethylene was interpreted as a result of fragmentation of the lamellar structure into small

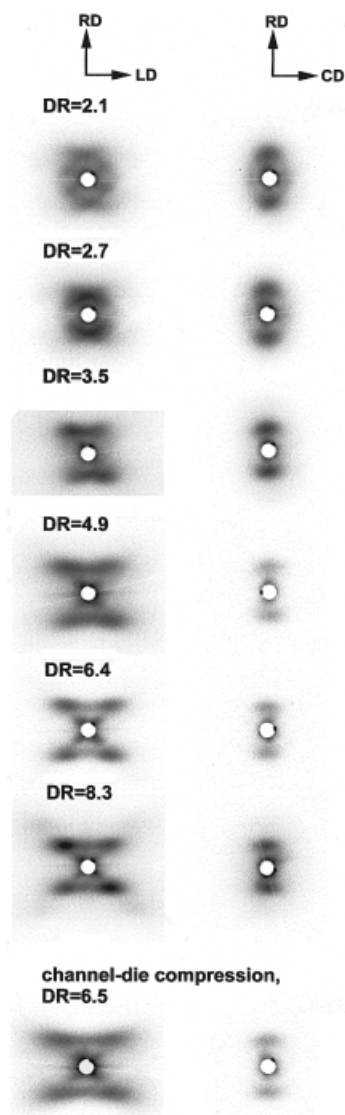


**Figure 9** 2D SAXS patterns obtained in LD and CD views for samples of PE-2 rolled at 110°C with a roll speed of 200 mm/min to the indicated DRs.

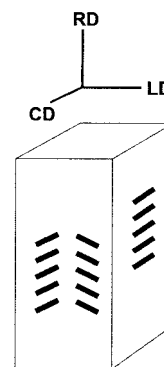


**Figure 10** Schematic illustration of the lamellar organization in rolled samples derived from the SAXS data.

blocks at a deformation of around 3.1 and the reconstitution of new lamellae from those blocks at higher deformation. Here, in rolled samples, the SAXS patterns suggest that the lamellar structure was preserved up to the highest DR studied, and no serious fragmentation occurred on deformation. The four-point patterns observed in the CD view indicate that the lamellae kinked, that is, broke only locally, but in a cooperative fashion, together with adjacent lamellae, and produced a chevronlike lamellar structure under observation from the CD direction. The orientation of the lamellar structure deduced from SAXS patterns of rolled samples is shown schematically in Figure 10.

The differences between the lamellar structures of rolled samples and those compressed in a channel die presented in ref. 7 can again be assigned to the differences in the molecular weights of the polyethylenes used. It must be noted here that the SAXS patterns revealed for ultrahigh molecular weight polyethylene in ref. 10 are also of the four-point type in contrast to conventional high-density polyethylene.<sup>7</sup> To confirm that the differences in the lamellar structures of the channel-die-compressed and rolled samples resulted from the differences in the molecular weights, we recorded the SAXS patterns of a PE-2 sample deformed in a channel die to DR = 6.5. These patterns are shown in the lowest row of Figure 9. They are quite similar to the patterns of rolled samples deformed to a similar strain. Therefore, it can be concluded that the evolution of the lamellar structure of rolled samples follows that of samples compressed in a channel die.

## CONCLUSIONS

Cavitation during plastic deformation greatly reduces the strength of oriented polymeric materials. Cavity-free deformation, such as plane-strain compression, leads to oriented polymeric materials with a strength much higher than that of a material oriented by deformation with no constraints imposed. In that defor-



mation mode, the side constraints imposed on the material during its compression help to prevent unwanted cavitation and to produce a material with a well-defined and sharp texture. The new method of rolling inside a channel reported here resembles to a large extent plane-strain compression in a channel die. It has been shown that the deformation processes of polyethylene by compression in a channel die and by rolling with side constraints proceed in very similar fashions. The rolling produces nearly plane-strain deformation, similar to channel-die compression. The crystalline texture and lamellar structure of polyethylene samples resulting from deformation from both methods are analogous at corresponding strains.

It can be expected that the mechanical properties of the deformed material, because of its high degree of orientation, should be equally good in materials deformed by either method. The method of rolling with side constraints described in this article has, however, a big advantage over other methods because it allows the continuous production of oriented materials of unlimited length. Moreover, rolling with side constraints seems to be better than conventional rolling, in which the relatively weak side constraints result merely from friction forces between the material and rolls, because in conventional rolling, the side constraints are the result of friction of the material along the roll only. It limits conventional rolling to the production of relatively thin sheets or films. In addition, unwanted fissures or cracks are frequently produced on edges of the rolled material. In contrast, constraint rolling allows for the production of bars or profiles with relatively large cross sections; in the laboratory

setup, we were able to produce long oriented bars with 12 mm × 12 mm cross sections. Such materials may become very attractive engineering materials with superior mechanical properties. The mechanical characterization of bars of rolled polyethylene is described in a companion article.<sup>19</sup>

## References

1. Ward, I. M.; Hadley, D. W. *Introduction to Mechanical Properties of Solid Polymers*; Wiley: New York, 1993.
2. Bowden, P. B.; Young, R. J. *J Mater Sci* 1974, 9, 2034.
3. *Plastic Deformation of Amorphous and Semicrystalline Materials*; Escaig, B.; G'Sell, C., Eds.; Editions de Physique: Paris, 1982.
4. Lin, L.; Argon, A. S. *J Mater Sci* 1994, 29, 294.
5. Galeski, A.; Argon, A. S.; Cohen, R. E. *Macromolecules* 1988, 21, 2761.
6. Peterlin, A. *Colloid Polym Sci* 1975, 253, 809.
7. Galeski, A.; Bartczak, Z.; Argon, A. S.; Cohen, R. E. *Macromolecules* 1992, 25, 5705.
8. Bellare, A.; Cohen, R. E.; Argon, A. S. *Polymer* 1993, 34, 1393.
9. Pluta, M.; Bartczak, Z.; Galeski, A. *Polymer* 2000, 41, 2271.
10. Boontongkong, Y.; Cohen, R. E.; Spector, M.; Bellare, A. *Polymer* 1998, 39, 6391.
11. Frank, F. C.; Keller, A.; O'Connor, A. *Philos Mag* 1958, 3, 64.
12. Yoda, O.; Kuriyama, I. *J Polym Sci Polym Phys Ed* 1977, 15, 773.
13. Krause, S. J.; Hosford, W. F. *J Polym Sci Polym Phys Ed* 1989, 27, 1867.
14. Bartczak, Z.; Galeski, A.; Morawiec, J.; Przygoda, M. *Pol. Pat. PL-178058* (1995).
15. Morawiec, J.; Bartczak, Z.; Kazmierczak, T.; Galeski, A. *Mater Sci Eng A* 2001, 317, 21.
16. Alexander, L. E. *X-Ray Diffraction Methods in Polymer Science*; Wiley-Interscience: New York, 1969.
17. Lewis, D.; Wheeler, E. J.; Maddams, W. F.; Preedy, J. E. *J Polym Sci Part A-2: Polym Phys* 1972, 10, 369.
18. Young, R. J.; Bowden, P. B. *Philos Mag* 1974, 29, 1061.
19. Bartczak, Z.; Morawiec, J.; Galeski, A. *J Appl Polym Sci* 2002.